Probing inter- and intrachain Zhang-Rice excitons in Li_2CuO_2 and determining their binding energy

Claude Monney,[1,2,*] Valentina Bisogni,[1,3,4] Ke-Jin Zhou,[1,5] Roberto Kraus,[4] Vladimir Strocov,[1] Günter Behr,[4] Stefan-Ludwig Drechsler,[4] Helge Rosner,[6] Steve Johnston,[7,8] Jochen Geck,[9] and Thorsten Schmitt[1,†]

[1] *Research Department Synchrotron Radiation and Nanotechnology, Paul Scherrer Institut, 5232 Villigen PSI, Switzerland*
[2] *Institute of Physics, University of Zurich, Winterthurerstrasse 190, 8057 Zurich, Switzerland*
[3] *National Synchrotron Light Source II, Brookhaven National Laboratory, Upton, NY 11973, USA*
[4] *Leibniz Institute for Solid State and Materials Research, Helmholtzstrasse 20, 01171 Dresden, Germany*
[5] *Diamond Light Source, Harwell Science and Innovation Campus, Didcot, Oxfordshire, OX11 0DE, United Kingdom*
[6] *Max-Planck Institute for Chemical Physics of Solids, 01187 Dresden, Germany*
[7] *Department of Physics and Astronomy, The University of Tennessee, Knoxville, TN 37996, USA*
[8] *Joint Institute for Advanced Materials, The University of Tennessee, Knoxville, Tennessee 37996, USA*
[9] *Chemistry and Physics of Materials, Paris Lodron University Salzburg, 5020 Salzburg, Austria*

arXiv:1609.08986v1 [cond-mat.str-el] 28 Sep 2016

Cuprate materials, like those hosting high temperature superconductivity, represent a famous class of materials where the correlations between the strongly entangled charges and spins produce complex phase diagrams. Several years ago the Zhang-Rice singlet was proposed as a natural quasiparticle in hole-doped cuprates. The occurance and binding energy of this quasiparticle, consisting of a pair of bound holes with antiparallel spins on the same CuO_4 plaquette, depends on the local electronic interactions, which are fundamental quantities for understanding the physics of the cuprates. Here, we employ state-of-the-art Resonant Inelastic X-ray Scattering (RIXS) to probe the correlated physics of the CuO_4 plaquettes in the quasi-one dimensional chain cuprate Li_2CuO_2. By tuning the incoming photon energy to the O K-edge, we populate bound states related to the Zhang-Rice quasiparticles in the RIXS process. Both intra- and interchain Zhang-Rice singlets are observed and their occurrence is shown to depend on the nearest-neighbor spin-spin correlations, which are readily probed in this experiment. We also extract the binding energy of the Zhang-Rice singlet and identify the Zhang-Rice triplet excitation in the RIXS spectra.

I. INTRODUCTION

As originally proposed by Zhang and Rice [1], a bound state formed by two holes on the same plaquette is a natural quasiparticle in hole-doped copper oxides. Called a Zhang-Rice (ZR) singlet in the case of opposite spins, this quasiparticle consists of a singlet pair of holes, where one is localized on the Cu^{2+} ion and the other is delocalized on surrounding ligand oxygens. In the undoped two-dimensional cuprates, the ZR singlet appears upon removing an electron from the CuO_4 plaquette [2]. In the doped case, recent experimental results have demonstrated that the ZR singlet remains stable in the ground state at all doping levels across the superconducting dome up to the metallic overdoped regime [3]. These findings confirm that the ZR singlet picture has a relevant role in the description of the electronic properties of the high-T_c cuprates at all dopings [4]. In addition, ZR singlet excitations have been observed in several one-dimensional corner-sharing cuprates by using electron spectroscopies [2, 5].

The existence of the ZRS has been also confirmed in the edge-sharing cuprate systems [6–8], with the use of RIXS [9–12] among other techniques. In particular, the ZR singlet has been predicted in these materials [13, 14], especially in the final state of the RIXS process [15], and has recently been observed in Li_2CuO_2 and $CuGeO_3$ [16].

There are two important energy scales for the creation of ZR excitations observed in undoped cuprate materials by RIXS: first, a hole has to be excited from the Cu site to an O site, which involves the charge transfer energy Δ. Second, the excited hole on the O site must bind to the hole on the central Cu site with a binding energy B_{ZR}. It is of great relevance to have direct experimental access to these quantities, as they are fundamental to the physics of correlated materials based on CuO_4 plaquettes.

We have chosen Li_2CuO_2 for investigating the physics of ZR quasiparticles in a simplified quasi-one-dimensional material. This prototypical realization of the edge-sharing chain cuprates is made out of CuO_4 plaquettes without apical oxygens. Despite its low dimensionality, this system develops long range magnetic order below $T_M = 9$ K, where collinear ferromagnetic (FM) intrachain correlations and alternating antiferromagnetic (AFM) interchain correlations are thought to be realized [17].

Here, we investigate the electronic excitations of Li_2CuO_2 with RIXS and X-ray absorption spectroscopy performed at the O K-edge [15, 18], revealing rich spectra showing peculiar charge transfer excitations. Distinct excitonic ZR singlet excitations are observed and are attributed to both intra- and interchain excitations.

* monney@physik.uzh.ch
† thorsten.schmitt@psi.ch

Their nature is further investigated by means of temperature dependent RIXS measurements. This method allows us to probe not only the nearest-neighbor (nn) intrachain magnetic correlations, but also the nn interchain magnetic correlations. Moreover, we also extract the ZR binding energy, B_{ZR}, from the energy loss position of the ZR singlet and the charge transfer energy Δ, which permits us to identify the ZR triplet excitonic excitation in the RIXS spectra. Finally, our results confirm the intrachain long-range ferromagnetic order and the interchain antiferromagnetic order in this material, emphasizing the capability of RIXS in probing short range magnetic correlations.

II. EXPERIMENTAL AND THEORETICAL DETAILS

A. RIXS experiment

Experiments were performed at the ADRESS beamline [19] of the Swiss Light Source, Paul Scherrer Institut, using the SAXES spectrometer [20]. RIXS spectra were typically recorded with a 2h acquisition time, achieving statistics of 100-150 photons on the peaks of interest (see below). A scattering angle of 130° was used and all the spectra were measured at the specular position (at an incidence angle of 65°), meaning that no momentum is transferred from the photons to the system along the chain direction. All spectra were acquired with $\sigma-$polarization of light. The combined energy resolution was 60 meV at the O K-edge ($\hbar\omega_i \sim 530$ eV). Li_2CuO_2 single crystals [21] (which are hygroscopic crystals) were cleaved in-situ at the pressure of about $5\cdot10^{-10}$ mbar and at 20 K, producing mirrorlike surfaces. The surface was oriented along the (101) direction, so that the CuO_4 plaquettes were 21° away from the surface. This means that the electric field of $\sigma-$polarized light was lying partially out of the plaquette plane, its main component in the plaquette being along the $c-$direction. All of the RIXS spectra presented here are normalized to the acquisition time, if not stated differently.

B. Density functional theory calculations

Scalar-relativistic density functional theory (DFT) electronic structure calculations were performed using the full-potential FPLO code [22], version fplo9.01-35. The parametrization of Perdew-Wang [23] was chosen for the exchange-correlation potential within the local density approximtion (LDA). The calculations were carried out on a well converged mesh of 1152 k-points in the first Brillouin zone to ensure a high accuracy for details in the electronic density of states. For the LDA+U calculations, the around-mean-field (AMF) double counting correction was applied. The calculations were carried out using the experimental crystal structure [24]. The value of U_{3d} used in the DFT calculations differs from the respective parameter U_{dd} in the cluster model: the U_{3d} is applied to all Cu-3d basis states in the DFT calculations, whereas the U_{dd} acts on the $3d_{xy}$ states in the core Hamiltonian of the pd-Hubbard model. Naturally, this requires a considerably smaller U_{3d}-value for the DFT calculations (including a slight basis dependence therein).

C. RIXS cluster calculations

XAS and RIXS calculations were carried out using the Kramers-Heisenberg formalism [18], where the initial, intermediate, and final states are obtained from small cluster exact diagonalization (ED). The calculation details are similar to those given in Ref. [16]. In order to model the interchain coupling, we considered a cluster formed from the two CuO_4 plaquettes with open boundary conditions that were bridged by a single Li atom. The unoccupied Li orbitals substantially increased the size of the Hilbert space. Our cluster therefore contained a limited orbital basis consisting of a single Cu $3d_{x^2-y^2}$ orbital on each Cu site, the O $2p_\sigma$ orbital on each oxygen site, and an effective $2s$ state on the Li site. The intra-plaquette Hamiltonian includes nearest-neightbor Cu-O and O-O hopping with $|t_{pd}| = 1$ and $|t_{pp}| = 0.65$ eV , respectively. The inter-plaquette O-Li hopping was taken to be $|t_{ps}| = 1$ eV. The onsite energies for the Cu, O, and Li orbitals were $\epsilon_d = 0$, $\epsilon_\sigma = 3.8$, and $\epsilon_s = -2$ eV, respectively. The on-site Hubbard interactions for the Cu $3d$ and O $2p$ orbitals were also included with $U_{dd} = 8$ and $U_{pp} = 4.1$ eV. All parameters are given in hole language.

The initial and final states were obtained for this cluster by diagonalizing the problem in the $N = 6$ hole sector with three spin up and three spin down holes. The intermediate states were found by diagonalizing in the $N = 5$ hole sector, with the inclusion of an additional core-hole potential $U_Q = 4$ eV on the oxygen site where the core hole was created. Finally, the reader should note that we have observed significant finite size effects in our previous work [16] for the RIXS spectra when we have performed calculations on smaller single-chain clusters. Therefore the RIXS spectra shown in the main text should be considered as a simple qualitative description of the system.

III. RESULTS AND DISCUSSION

A. RIXS spectra

During a RIXS experiment performed at the O K-edge, light excites directly an electron from an O $1s$ core state into an O $2p$ valence state. However, due to the hybridization of the O $2p$ states with the Cu $3d$ states in the CuO_4 plaquettes, the excited electron can also fill a Cu $3d$ state. Such a process can lead to the creation of an ZR exciton on a plaquette as a final state. This is illustrated in Fig. 1 (a). Starting from an initial state with

two neighboring CuO_4 plaquettes on a single chain with both Cu in a d^9 configuration, written in short (d^9, d^9), a RIXS intermediate state $(d^9, \underline{1s}\, d^{10})$ (with one hole in the O 1s states, $\underline{1s}$) is reached, deexciting afterwards to a final state $(d^9\underline{L}, d^{10})$ ($\underline{L}$ denotes a ligand hole). Comparing the initial to the final state, one sees that a non-local charge-transfer has occurred from one plaquette to another [25], leading to an excitonic excitation due to the local charge imbalance [6]. From the conservation of spin in the process, an initial state with antiparallel spins (panel (a)) on the neighboring plaquettes ends up in a final state with two holes having antiparallel spins on the left plaquette, $d^9\underline{L}$, which is a ZR singlet [1]. It is straightforward to conclude that an initial state with parallel spins on the neighboring plaquettes will give rise to a ZR triplet.

In Li_2CuO_2 and other spin-chain cuprates, there is another possibility for the creation of a low-energy ZR singlet excitation, which takes place between two neighboring CuO_2 chains, as illustrated in Fig. 1 (b). In Li_2CuO_2, the donor Li atoms lie between such chains [26, 27] and can act as a bridge for the electron created at the O site in the intermediate state of the RIXS process. This results in the creation of an interchain ZR singlet exciton in the final state.

In the first part of our experimental approach, we measured X-ray absorption spectroscopy (XAS) at the O K edge on Li_2CuO_2 samples, in order to determine the appropriate incident photon energy for RIXS. In Fig. 2 (right), we show the XAS spectrum obtained at 20 K (which is above T_M). It is composed of two main peaks. The peak at 529.7 eV is due to the upper Hubbard band (UHB) consisting mainly of Cu $3d_{x^2-y^2}$ states hybridized with O $2p$ states of the same symmetry [28]. Next to this sharp line, there is another broad structure extending from about $\hbar\omega_i$ = 531 eV to 534 eV, with a maximum at 532 eV. This structure is due to Li $2s/2p$ states hybridized with (in-chain) O states. This interpretation of the XAS features is verified by our density functional theory (DFT) calculations shown in Fig. 3 (a) (see below). The character of the low-energy unoccupied states and their energy scale compare well with our XAS spectrum.

The final states of the XAS spectrum described above correspond to intermediate states in the RIXS process [18, 29]. Specifically, by tuning the incoming photon energy along the XAS spectrum of Li_2CuO_2, as shown by the arrows on Fig. 2 (right), we select which intermediate states are involved in the RIXS process. The resulting O K-edge RIXS spectra measured also at 20 K are plotted in an energy loss scale in Fig. 2 (left). At first sight, one recognizes remarkably rich spectra, exhibiting different sharp peaks.

The intense broad structure between 4 and 10 eV originates from higher-energy charge transfer excitations. Most of this spectral weight disperses as a function of the incident photon energy above $\hbar\omega_i$ =531 eV, identifying a significant amount of these excitations as fluorescence, coming from the valence states that have a mixed Cu-

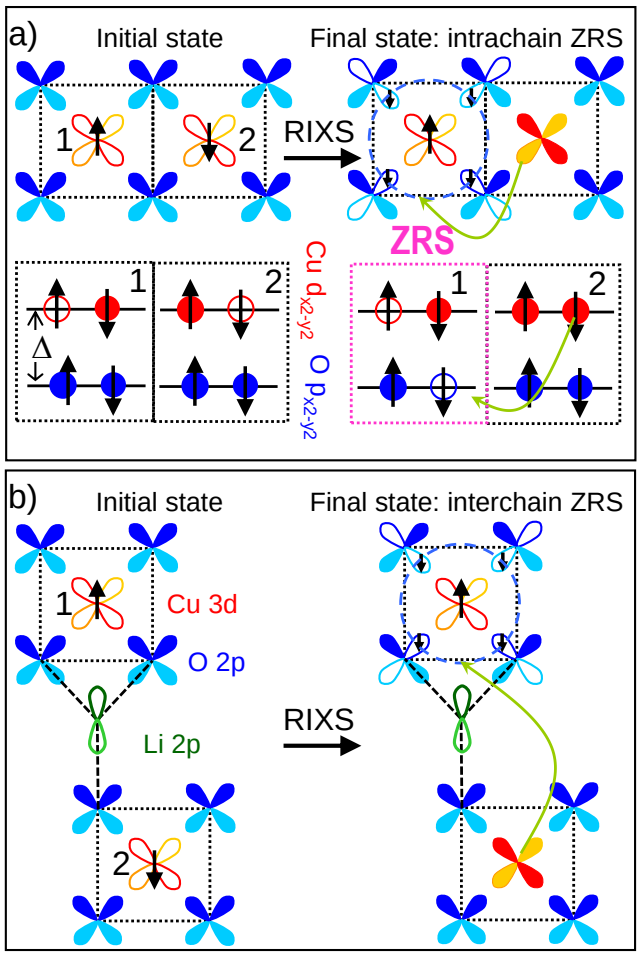

FIG. 1. Schematic pictures of the creation of the ZR singlet (ZRS) excitons in the RIXS process. (a) Comparison of the RIXS initial and final states for the intrachain ZR singlet exciton, together with the corresponding energetic diagram. Full and empty symbols represent filled and empty states/orbitals. (b) A similar picture is shown for the case of the interchain ZR singlet exciton, for which the Li atom acts as a bridge between neighboring chains. The green arrow indicates the hole transfer between two plaquettes leading to excitonic excitations.

O character according to first-principle calculations [30]. More interesting are the peaks situated between the elastic line (at 0 energy loss) and the higher-energy charge transfer excitations. Two sharp peaks appear at about 2 eV and do not move in energy loss as a function of incident energy – they exhibit a so-called Raman behavior. This behavior (and the involved energy scale, which is in rather good agreement with quantum chemistry calculations [31]) is typical of local excitations occuring between the different d-orbitals of a single Cu site, called $dd-$excitations. This is supported by the fact that they resonate when the incident energy is tuned to the UHB, as already observed by Learmonth *et al.* [9].

Our main interest relates to the Raman excitations observed at energy losses between the $dd-$excitations and

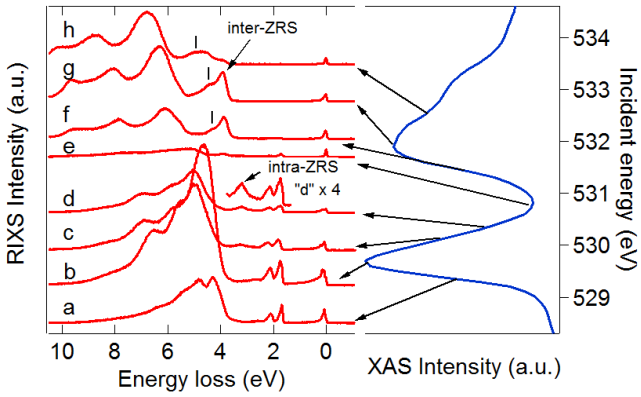

FIG. 2. Incident energy dependence of the RIXS spectra. (Right) XAS spectrum measured at the O K-edge on Li_2CuO_2 with $\sigma-$polarized light and at 20 K, (left) together with the corresponding RIXS spectra (on an energy loss scale) measured at incident photon energies given by the arrows relative to the XAS spectrum energy scale. The position of the intra- and interchain ZR singlet excitations are emphasized by arrows. The position of the possible dispersive ZR fluorescence excitation is also shown by vertical lines. (see text).

the higher-energy charge transfer excitations. An interesting peak appears (in spectra c, d of Fig. 2) at about 3.2 eV energy loss when selecting incident photon energies corresponding to exciting the O $1s$ electron into the UHB (around $\hbar\omega_i$ =530.1 eV). We have already identified this RIXS peak as the intrachain ZR singlet exciton [16]. Furthermore, by tuning the incident photon energy to the Li-hybridized XAS structure (around $\hbar\omega_i$ =531.9 eV), we create RIXS-intermediate states, where the O $1s$ electron is excited into Li-hybridized states. In this case, another Raman contribution appears (in spectra f, g, h of Fig. 2) at about 4.0 eV energy loss. We will show now that it corresponds to the interchain ZR singlet exciton.

B. Calculations

To better understand the structure of the XAS spectrum we have performed DFT calculations to determine the nature of the unoccupied states in Li_2CuO_2. In order to account for the strong electron-electron interaction in this material, we introduced an orbital dependent Coulomb repulsion U_{3d} at the Cu site, varying between 5.0 and 6.0 eV. This range for U_{3d} is known empirically to describe well the magnetic properties due to the Heisenberg exchange between the localized Cu-moments in many Cu-O compounds [17, 32, 33]. The calculated density of states (DOS) is shown in Fig. 3 (a) and is compared to the XAS spectrum in Fig. 2 as a first approximation. With $U_{3d} = 5.5$ eV, the DOS obtained here reproduces well the two peaks observed in the XAS (Fig. 2, right). The partial DOS shown in Fig. 3 (a) confirms that the second peak (at higher energies) in the DOS is mostly due to O $2p$ states hybridized with Li $2p$, in agreement with a previous XAS study [28]. This supports the idea that an electron is promoted into such Li $2p$ hybridized states in the intermediate state of RIXS when the incident energy is tuned at about 532 eV, i.e. 1.5 eV above the upper Hubbard band (see Fig. 2).

We now show that an electron excited with an incident energy of about 532 eV can exploit the unoccupied Li $2p$ states to travel from one CuO_2 chain to the neighboring one. For this purpose, we have calculated RIXS intensities at the O K-edge using a small cluster ED calculation based on a model system consisting of two CuO_4 plaquettes bridged by a Li atom (as in Fig. 1 (b)). Such a dual-chain geometry involving many different electronic orbitals has never been used for such calculations so far. (For example, in our previous work [16], we have simulated a single CuO_2 chain with up to 5 CuO_4 plaquettes.)

The ED results for the RIXS spectrum is shown in Fig. 3 (b), while the corresponding XAS spectrum is shown in the inset. The XAS spectrum reproduces well the two main peaks of the measured XAS, given the simplicity of the model system. The RIXS spectrum has been calculated for an incident energy tuned to the second peak in the XAS (see the red arrow in the inset in Fig. 3 (b)). In addition to the elastic line at 0 eV energy loss, a series of charge transfer excitations appear above 6 eV energy loss, in agreement with the experiment (see Fig. 2 (left)). Most interestingly, the calculation displays another peak at about 4.8 eV energy loss. This corresponds to a $d^9\underline{L}$ state, where a hole has been transferred from one CuO_2 chain to the other during the RIXS process. This excitation therefore corresponds to the interchain ZR singlet exciton, which is excited when the incident energy is tuned to Li-O hybridized intermediate states. While the energy of this RIXS excitation is somewhat larger than what is experimentally observed (4.0 eV) due to the simplicity of the model adopted here, this calculation together with the DOS shown above, demonstrates that it is possible to create an interchain ZR singlet exciton at the O K-edge in Li_2CuO_2.

C. Temperature dependence

The conservation of spin in this RIXS process allows us to determine the local spin correlations by looking at the ZR exciton intensity in the RIXS data as a function of temperature (see also Fig. 1) [16]. Having this in mind, we have measured the temperature dependence of the RIXS intensity of both the intrachain and the interchain ZR singlet exciton peak at 3.2 eV and 4.0 eV energy loss, see Fig. 4 (a) and (b) respectively. The spectra zoomimg on the intrachain and the interchain ZR exciton peaks are shown in Fig. 4 (c) and (d), respectively. The temperature dependence of these two Raman-like peaks is opposite, as summarized in the inset of Fig. 4 (c), which shows the integrated peak intensities vs temperature: the interchain ZR singlet exciton is increasing in

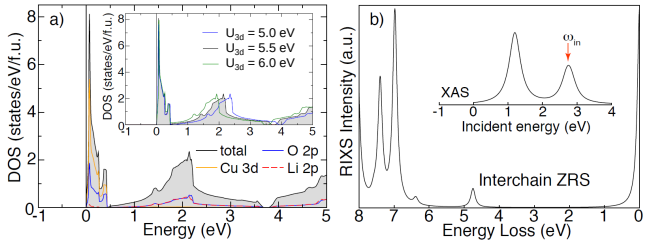

FIG. 3. DFT and RIXS cluster calculations. (a) Calculated DOS within DFT+U for the unoccupied states of Li_2CuO_2. The main panel shows the orbital-resolved DOS of Li_2CuO_2 for $U_{3d} = 5.5$ eV. The inset shows the variation in the total DOS for different values of U_{3d} (the 0 eV reference energy is placed at the lower band edge of the unoccupied states). (b) Calculated XAS (inset) and RIXS for a ED cluster calculation based on a 2 CuO_4 plaquettes bridged by a Li atom. The red arrow indicates at which incident energy the RIXS spectrum has been calculated.

intensity when temperature is lowered, while the intrachain ZR singlet exciton is decreasing in intensity.

These temperature behaviors allow us now to relate the nature of these ZR singlet excitons to the magnetic correlations. As mentioned above, while long-range FM order occurs in the CuO_2 chains of Li_2CuO_2 below the critical temperature, $T_M = 9$ K, long-range AFM order develops across the chains [17]. Above T_M, the magnetic order along the chains is expected to vanish, transforming into short range order of decreasing correlation length as temperature increases. As a consequence, parallel spins are dominating the intrachain nearest neighbor spin correlations at low temperatures, but their occurence decreases as temperature increases. This is consistent with the temperature dependence of the intrachain ZR singlet peak in Fig. 4 (c), the intensity of which decreases as the temperature decreases. Similarily, the development of interchain AFM order at low temperatures increases the probability of finding antiparallel spins on neighboring chains. Thus, the intensity of the interchain ZR singlet increases as the temperature is decreased, as shown in Fig. 4 (d). More generally, this observation confirms that O K-edge RIXS is capable of probing the short-range magnetic correlations of such low dimensional systems.

D. Singlets and triplets

As expected from our schematic description in Fig. 1, we observe both the intra- and interchain ZR singlet excitons in our RIXS data on Li_2CuO_2. Comparing the energy loss of these peaks allows us to gain substantial physical information on the ZR physics in this prototypical low dimensional cuprate. First, following the processes depicted in Fig. 1, we estimate the energy cost of such an excitation, starting from a (d^9, d^9) configuration (charge neutral). The transfer of a hole from a Cu $d_{x^2-y^2}$ orbital to ligand $p_{x^2-y^2}$ orbitals of the neighboring CuO_4 plaquette costs the charge transfer energy, Δ. (We can neglect the cost of the broken magnetic bonds in comparison to this energy scale in the case of edge-shared geometry since the Cu-Cu exchange energies are less than 20 meV [14, 17].) As explained above, this RIXS final state is now $(d^9\underline{L}, d^{10})$, meaning that charge has been transferred from one plaquette to another, leading to the creation of an electron-hole bound state between two plaquettes forming an exciton. This excitonic contribution to the energy cost is contained already in the Coulombic part of the charge transfer energy [34]. As a consequence, we distinguish between the interchain Δ_{inter} and intrachain Δ_{intra} charge transfer energies, due to the different distances between the hole and the electron of the exciton in these two processes. The energy loss of the ZR excitation in the RIXS process is given by $E^{(s,t)}_{inter,intra} = \Delta_{inter,intra} - B^{(s,t)}_{ZR}$, with $B^{(s,t)}_{ZR}$ being the binding energy of the ZR state, which can be singlet (s) or triplet (t). In other words, the binding energy of the ZR excitation is defined as the energy difference between the charge transfer energy Δ and its excitation energy (which is smaller than Δ). We define additionally the energy splitting between the ZR singlet and ZR triplet excitons as $\Delta E_{ZR} = B^{(t)}_{ZR} - B^{(s)}_{ZR}$.

We recently evaluated the intrachain charge transfer energy in Li_2CuO_2 to be $\Delta_{intra} = 4.6$ eV by comparing RIXS spectra with calculations done on a multiplaquette CuO_2 chain [35]. Together with the excitation energy of the intrachain ZR singlet, $E^{(s)}_{intra} = 3.2$ eV, this gives us a ZR singlet binding energy of $B^{(s)}_{ZR} = 1.4$ eV in Li_2CuO_2. This is a first important result. This ZR singlet binding energy must be the same for the interchain ZR singlet, since the plaquettes where the ZR singlet takes place in the final state of the RIXS process, are the same. From the excitation energy of the interchain ZR singlet, $E^{(s)}_{inter} = 4.0$ eV, we infer then an interchain charge transfer energy of $\Delta_{inter} = 5.4$ eV, which is 0.8 eV higher than the intrachain one. This energy difference is probably coming from the different contribution of the nearest-neighbor Coulomb interaction U_{pd} in the final state of the intrachain vs. interchain charge transfer (i.e. in the excitonic contribution).

Having identified intrachain and interchain ZR singlet, we now turn to the ZR triplet excitations. For this purpose, we show in Fig. 4 the RIXS spectra of Li_2CuO_2 measured on a 10 eV range for incident energies of (a) $\hbar\omega_i$ =530.1 eV and (b) $\hbar\omega_i$ =531.9 eV corresponding to exciting intrachain and interchain ZR excitons, respectively. For $B^{(s)}_{ZR} = 1.4$ eV, we expect the spin singlet to lie at an energy $\Delta - 3\Delta E_{ZR}/4$ and the spin triplet at an energy $\Delta + 1\Delta E_{ZR}/4$ with respect to the charge transfer energy, as illustrated schematically in Fig. 4 (e) and (f). Additionally, the ZR triplet exciton must have the inverse temperature behavior as that of the ZR singlet. Consequently, the ZR triplet should be located at about $B^{(t)}_{ZR} = 0.47$ eV above the charge transfer energy, involving an energy separation $\Delta E_{ZR} = 1.87$ eV between the

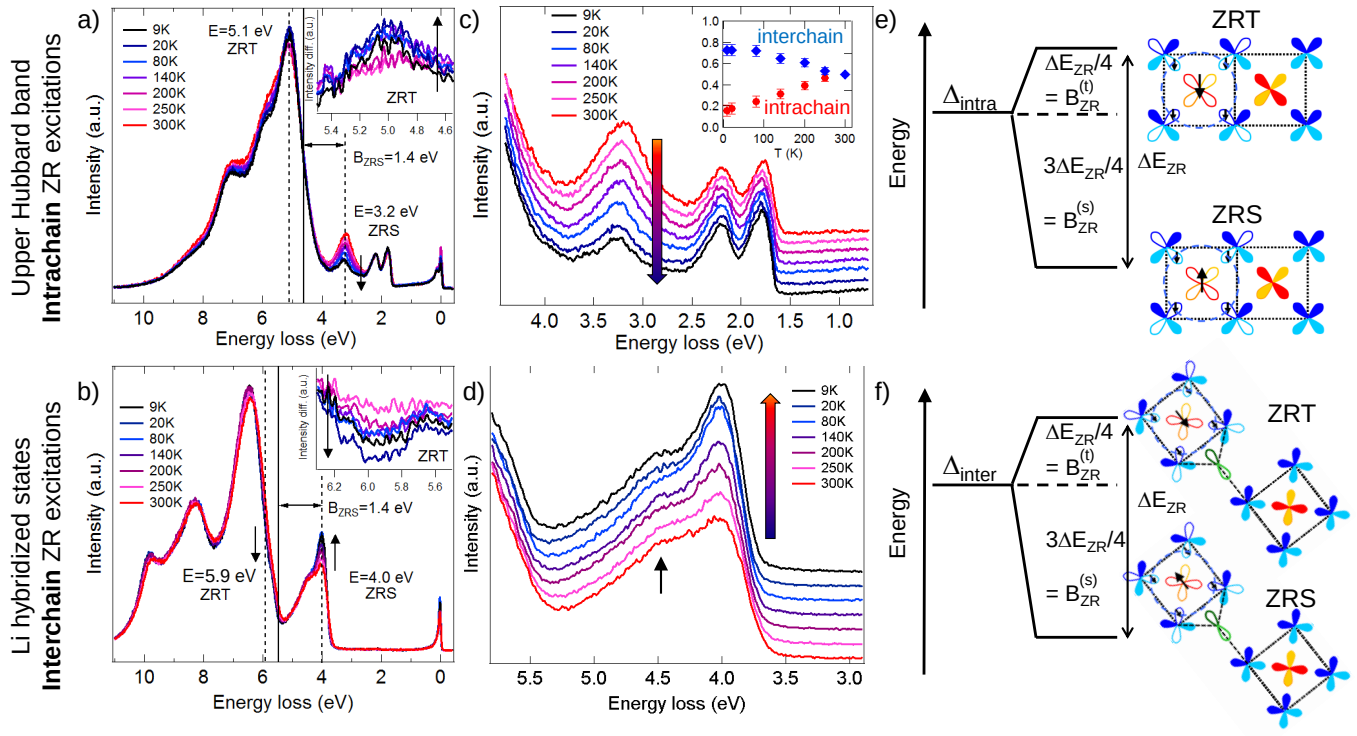

FIG. 4. Temperature dependence of RIXS intensities of the intrachain and interchain ZR singlet excitations. RIXS spectra measured as a function of temperature at the O K-edge of Li_2CuO_2, with σ-polarization of light and an incident energy of (a) $\hbar\omega_i$ =530.1 eV (on the edge of the UHB) and of (b) $\hbar\omega_i$ =531.9 eV (on the Li-hybridized states). The RIXS spectra in (a) are normalized to the total intensity area of the *dd*-excitations [16]. In (a) and (b), the insets show difference RIXS spectra, for which the spectrum at 300 K has been subtracted and the vertical continuous line indicate the energy position of the charge transfer energies $\Delta_{inter,intra}$ (see text). (c) and (d): corresponding zoom on the ZR singlet excitons. The spectra are shifted in intensity by a constant offset for better visibility. (c) The inset shows the integrated RIXS intensity (normalized to 0.5 at room temperature) of the ZR singlet excitons as a function of temperature. Schematic energy scale for the (e) intrachain and (f) interchain ZR excitons, depicting how the ZR singlet excitation energy is shifted to energy losses lower than the charge transfer energy, Δ, by its binding energy, $B_{ZR}^{(s)}$, while the ZR triplet (ZRT) excitation energy is shifted above Δ. The splitting between the ZR singlet and ZR triplet excitation energies is ΔE_{ZR}.

ZR singlet and the ZR triplet [**?**]. This energy scale has been confirmed from the singlet/triplet splitting obtained for two holes on a single CuO_4 plaquette with open boundary conditions (not shown here). In the case of the intrachain ZR excitons, the ZR triplet should be located at about 5.1 eV energy loss. At this energy in Fig. 4 (a) (vertical dashed line), we see a large peak, the intensity of which has a temperature behavior opposite to that of the intrachain ZR singlet (vertical arrows). We identify this excitation as the intrachain ZR triplet exciton. In a similar way, we expect to see the interchain ZR triplet exciton at about 5.9 eV energy loss. In the RIXS spectrum of Fig. 4 (b), we do not distinguish a clear peak, but closer inspection (see inset) reveals a small shoulder, the intensity of which is decreasing with decreasing temperature, as expected for an excitation suppressed by interchain antiferromagnetic correlations. We tentatively identify this excitation as the interchain ZR triplet exciton. More generally, our analysis shows that the identification in RIXS data of the ZR singlet and ZR triplet excitons permits us to directly extract ΔE_{ZR} from their energy splitting. This, in turn, delivers the value of the ZR binding energies, $B_{ZR}^{(s,t)}$, as shown schematically in Fig. 4 (e) and (f).

Finally, we comment on the work of Learmonth *et al.* [9] in the light of our new results. There, the authors tentatively attributed to a ZR triplet excitation a shoulder at 4.1 eV energy loss near the fluorescence, resonating on a large incident energy range around the UHB. Here, we identify this excitation as the interchain ZR singlet excitation, as it clearly resonates at higher incident energies. We attribute this discrepancy in the interpretation to the higher energy resolution and statistics of our experiment,as well as the fact that no temperature dependent study could be performed in Ref. [9]. In Ref. [9] the intrachain ZR singlet was not observed, as the corresponding incident energy (slightly detuned from the UHB) was not used. Interestingly, a ZR singlet fluorescence excitation was proposed for describing a fluorescence-like excitation developing at incident energies tuned to the Li-O hybridized states in the XAS. Due to our higher energy

resolution, we can distinguish here this possible excitation (located by an arrow in Fig. 4 (d), at about 4.5 eV, and by vertical lines in Fig. 2 (left)) from the interchain ZR singlet exciton. Furthermore, it does not display any temperature dependence, confirming Learmonth *et al.*'s assumption [9].

IV. CONCLUSIONS

We have performed Resonant Inelastic X-ray Scattering measurements at the O K-edge on the edge-sharing chain cuprate, Li_2CuO_2. Rich RIXS spectra are observed with specific charge transfer excitations, which are understood as Zhang-Rice singlet and triplet excitons created in the final state of the RIXS process. By analysing the character of the states involved in the final states of the X-ray absorption spectra and thus in the intermediate states of the RIXS spectra, we identify interchain ZR exciton excitations. These are confirmed by RIXS cluster calculations. Both the intrachain and interchain ZR excitations are measured as a function of temperature and their strong temperature dependent behavior is intimately related to intrachain and interchain nearest neighbor magnetic correlations. This permit us, using RIXS, to confirm in Li_2CuO_2 the development of both intrachain ferromagnetic order and interchain antiferromagnetic order at low temperature. The corresponding ZR triplet excitons are also observed in the RIXS spectra. With this work, we demonstrate how it is possible to estimate several fundamental quantities including the ZR singlet binding energy, as well as interchain and intrachain charge transfer energies, from the energy loss position of these excitonic excitations.

V. ACKNOWLEDGMENTS

We acknowledge fruitful discussions with H.M. Rønnow, U. Staub, J. van der Brink, J. Málek, R. Kuzian and K. Wohlfeld. S.L.D. thanks A.Boris and D.Efremov for discussions of the role of interchain ZR excitons. The experimental part of this work was performed at the ADRESS beamline of the Swiss Light Source at the Paul Scherrer Institut, Switzerland. This project was supported by the Swiss National Science Foundation and its National Centre of Competence in Research MaNEP. This research has been jointly funded by the German Science Foundation and the Swiss National Science Foundation within the D-A-CH program (SNSF Grant No. $200021L_141325$ and DFG Grant No. GE $1647/3-1$). C.M. gratefully acknowledges the support by the SNSF under grant $PZ00P2_154867$. S.J. is supported by the University of Tennessees Science Alliance Joint Directed Research and Development (JDRD) program, a collaboration with Oak Ridge National Laboratory. J.G. gratefully acknowledges the support by the Collaborative Research Center SFB 1143.

[1] F.C. Zhang and T.M. Rice, *Effective Hamiltonian for the superconducting Cu oxides*, Phys. Rev. B **37**, 3759 (1988).

[2] L.H. Tjeng, B. Sinkovic, N.B. Brookes, J.B. Goedkoop, R. Hesper, E. Pellegrin, F.M.F. de Groot, S. Altieri, S.L. Hulbert, E. Shekel and G.A. Sawatzky, *Spin-Resolved photoemission on anti-ferromagnets: Direct observation of Zhang-Rice singlets in CuO*, Phys. Rev. Lett. **78**, 1126 (1997).

[3] N. B. Brookes, G. Ghiringhelli, A.-M. Charvet, A. Fujimori, T. Kakeshita, H. Eisaki, S. Uchida, and T. Mizokawa, *Stability of the Zhang-Rice singlet with doping in Lanthanum Strontium Copper oxide across the superconducting dome and above*, Phys. Rev. Lett. **115**, 027002 (2015).

[4] C.-C. Chen, M. Sentef, Y. F. Kung, C. J. Jia, R. Thomale, B. Moritz, A. P. Kampf and T. P. Devereaux, *Doping evolution of the oxygen K-edge x-ray absorption spectra of cuprate superconductors using a three-orbital Hubbard model*, Phys. Rev. B **87**, 165144 (2013).

[5] R. Neudert, M. Knupfer, M.S. Golden, J. Fink, W. Stephan, K. Penc, N. Motoyama, H. Eisaki and S. Uchida, *Manifestation of spin-charge separation in the dynamic dielectric response of one-dimensional Sr_2CuO_3*, Phys. Rev. Lett. **81**, 657 (1998).

[6] Y. Matiks, P. Horsch, R.K. Kremer, B. Keimer and A.V. Boris, *Exciton doublet in the Mott-Hubbard insulator $LiCuVO_4$ identified by spectral ellipsometry*, Phys. Rev. Lett. **103**, 187401 (2009).

[7] S. Atzkern, M. Knupfer, M. S. Golden, J. Fink, C. Waidacher, J. Richter, and K. W. Becker, N. Motoyama, H. Eisaki, and S. Uchida, *Dynamics of a hole in a CuO_4 plaquette: Electron energy-loss spectroscopy of Li_2CuO_2*, Phys. Rev. B **62**, 7845 (2000).

[8] Y. Matiks, *Spectroscopic ellipsometry of spin-chain cuprates and $LaNiO_3$-based heterostructures*, PhD thesis, University of Stuttgart, 2011.

[9] T. Learmonth, C McGuinness, P.-A. Glans, J.E. Downes, T. Schmitt, L.-C. Duda, J.-H. Guo, F.C. Chou and K.E. Smith, *Observation of multiple Zhang-Rice excitations in a correlated solid: Resonant inelastic X-ray scattering study of Li_2CuO_2*, Euro. Phys. Lett. **79**, 47012 (2007).

[10] Y.-J. Kim, J. P. Hill, F. C. Chou, D. Casa, T. Gog, and C. T. Venkataraman, *Charge and orbital excitations in Li_2CuO_2*, Phys. Rev. B **69**, 155105 (2004).

[11] L.-C. Duda, J. Downes and C. McGuinness, T. Schmitt and A. Augustsson, K. E. Smith, G. Dhalenne and A. Revcolevschi, *Bandlike and excitonic states of oxygen in CuGeO3: Observation using polarized resonant soft-x-ray emission spectroscopy*, Phys. Rev. B **61**, 4186 (2000).

[12] F. Vernay, B. Moritz, I. S. Elfimov, J. Geck, D. Hawthorn, T. P. Devereaux and G. A. Sawatzky, *Cu K-edge resonant inelastic x-ray scattering in edge-sharing cuprates* , Phys. Rev. B **77**, 104519 (2008).

[13] K. Okada and A. Kotani, *Copper-related information from the oxygen 1s resonant x-ray emission in low-dimensional cuprates*, Phys. Rev. B **65**, 144530 (2002).

[14] J. Málek, S.-L. Drechsler, U. Nitzsche, H. Rosner and H. Eschrig, *Temperature-dependent optical conductivity of undoped cuprates with weak exchange*, Phys. Rev. B **78**, 060508(R) (2008).

[15] K. Okada and A. Kotani, *Zhang-Rice singlet-state formation by oxygen 1s resonant x-ray emission in edge-sharing copper-oxide systems*, Phys. Rev. B **63**, 045103 (2001).

[16] C. Monney, V. Bisogni, K.J. Zhou, R. Kraus, V.N. Strocov, G. Behr, J. Málek, R. Kuzian, S.-L. Drechsler, S. Johnston, A. Revcolevschi, B. Buchner, H.M. Ronnow, J. van den Brink, J. Geck, T. Schmitt, *Determining the short-range spin correlations in the spin-chain Li_2CuO_2 and $CuGeO_3$ compounds using resonant inelastic x-ray scattering*, Phys. Rev. Lett. **110**, 087403 (2013).

[17] W.E.A. Lorenz, R.O. Kuzian, S.-L. Drechsler, W.-D. Stein, N. Wizent, G. Behr, J. Málek, U. Nitzsche, H. Rosner, A. Hiess, W. Schmidt, R. Klingeler, M. Loewenhaupt and B. Bchner, *Highly dispersive spin excitations in the chain cuprate Li_2CuO_2*, Euro. Phys. Lett. **88**, 37002 (2009).

[18] L. J. P. Ament, M. van Veenendaal, T. P. Devereaux, J. P. Hill, J. van den Brink, *Resonant inelastic x-ray scattering studies of elementary excitations*, Rev. Mod. Phys. **83** 705 (2011).

[19] V.N. Strocov, T. Schmitt, U. Flechsig, T. Schmidt, A. Imhof, Q. Chen, J. Raabe, R. Betemps, D. Zimoch, J. Krempasky, X. Wang, M. Grioni, A. Piazzalunga and L. Patthey, *High-resolution soft x-ray beamline ADRESS at the Swiss Light Source for resonant inelastic x-ray scattering and angle-resolved photoelectron spectroscopies*, J. Synchrotron Rad. **17**, 631 (2010).

[20] G. Ghiringhelli, A. Piazzalunga, C. Dallera, G. Trezzi, L. Braicovich, T. Schmitt, V.N. Strocov, R. Betemps, L. Patthey, X. Wang and M. Grioni, *SAXES, a high resolution spectrometer for resonant x-ray emission in the 4001600 eV energy range*, Rev. Sci. Instrum. **77**, 113108 (2006).

[21] N. Wizent, G. Behr, W. Löser, B. Büchner and R. Klingeler, *Challenges in the crystal growth of Li_2CuO_2 and $LiMnPO_4$*, J. Cryst. Growth **318**, 995 (2011).

[22] K. Koepernik, and H. Eschrig, *Full-potential nonorthogonal local-orbital minimum-basis band-structure scheme*, Phys. Rev. B 59, 1743 (1999); I. Opahle, K. Koepernik, and H. Eschrig, *Full-potential band-structure calculation of iron pyrite*, Phys. Rev. B **60**, 14035 (1999); http://www.fplo.de.

[23] J.P. Perdew and Y. Wang, *Accurate and simple analytic representation of the electron-gas correlation energy*, Phys. Rev. B **45**, 13244 (1992).

[24] F. Sapina, J. Rodriguez Carvajal, M.J. Sanchis, R. Ibanez, A. Beltran, and D. Beltran, *Crystal and magnetic structure of Li_2CuO_2*, Solid State Communications **74**, 779-784 (1990).

[25] L.-C. Duda, T. Schmitt, M. Magnuson, J. Forsberg, A. Olsson, J. Nordgren, K. Okada and A. Kotani, *Resonant inelastic x-ray scattering at the oxygen K resonance of NiO: Nonlocal charge transfer and double-singlet excitations*, Phys. Rev. Lett. **96**, 067402 (2006).

[26] Y. Mizuno, T. Tohyama and S Maekawa, *Interchain interactions and magnetic properties of Li_2CuO_2*, Phys. Rev. B **60**, 6230 (1999).

[27] R. Hoppe and H. Rieck, *Die Kristallstruktur von Li_2CuO_2*, Z. anorg. allg. Chem. **379**, 157 (1970).

[28] R. Neudert, H. Rosner, S.-L. Drechsler, M. Kielwein, M. Sing, Z. Hu, M. Knupfer, M.S. Golden, J. Fink, N. Nucker, M. Merz, S. Schuppler, N. Motoyama, H. Eisaki, S. Uchida, M. Domke and G. Kaindl, *Unoccupied electronic structure of Li_2CuO_2*, Phys. Rev. B. **60**, 13413 (1999).

[29] A. Kotani and S. Shin, *Resonant inelastic x-ray scattering spectra for electrons in solids*, Rev. Mod. Phys. **73**, 203 (2001).

[30] R. Weht and W.E. Pickett, *Extended moment formation and second neighbor coupling in Li_2CuO_2*, Phys. Rev. Lett. **81**, 2502 (1998).

[31] H.-Y. Huang, N.A. Bogdanov, L. Siurakshina, P. Fulde, J. van den Brink and L. Hozoi, *Ab initio calculation of d-d excitations in quasi-one-dimensional Cu d^9 correlated materials*, Phys. Rev. B **84**, 235125 (2011).

[32] M. Schmitt, J. Málek, S.-L. Drechsler, and H. Rosner, *Electronic structure and magnetic properties of Li_2ZrCuO_4: A spin-1/2 Heisenberg system close to a quantum critical point*, Phys. Rev. B **80**, 205111 (2009)

[33] A.U.B. Wolter, F. Lipps, M. Schäpers, S.-L. Drechsler, S. Nishimoto, R. Vogel, V. Kataev, B. Büchner, H. Rosner, M. Schmitt, M. Uhlarz, Y. Skourski, J. Wosnitza, S. Süllow, and K. C. Rule, *Magnetic properties and exchange integrals of the frustrated chain cuprate linarite $PbCuSO_4(OH)_2$*, Phys. Rev. B **85**, 014407 (2012)

[34] Y. Ohta, T. Tohyama and S. Maekawa, *Apex oxygen and critical temperature in copper oxide superconductors: Universal correlation with the stability of local singlets*, Phys. Rev. B **43**, 2968 (1991).

[35] S. Johnston, C. Monney, V. Bisogni, K.-J. Zhou, Ro. Kraus, G. Behr, V. N. Strocov, J. Málek, S.-L. Drechsler, J. Geck, T. Schmitt, J. van den Brink, *Electron-lattice interactions strongly renormalize the charge transfer energy in the spin-chain cuprate Li_2CuO_2*. Nature Commun. **7**, 10653 (2016).